

# Strong coupling between single-electron tunneling and nano-mechanical motion

G. A. Steele<sup>1</sup>, A. K. Hüttel<sup>1,\*</sup>, B. Witkamp<sup>1</sup>, M. Poot<sup>1</sup>, H. B. Meerwaldt<sup>1</sup>, L. P. Kouwenhoven<sup>1</sup>  
and H. S. J. van der Zant<sup>1</sup>

<sup>1</sup>*Kavli Institute of NanoScience, Delft University of Technology, PO Box 5046, 2600 GA, Delft, The Netherlands.*

## Abstract

Nanoscale resonators that oscillate at high frequencies are useful in many measurement applications. We studied a high-quality mechanical resonator made from a suspended carbon nanotube driven into motion by applying a periodic radio frequency potential using a nearby antenna. Single-electron charge fluctuations created periodic modulations of the mechanical resonance frequency. A quality factor exceeding  $10^5$  allows the detection of a shift in resonance frequency caused by the addition of a single-electron charge on the nanotube. Additional evidence for the strong coupling of mechanical motion and electron tunneling is provided by an energy transfer to the electrons causing mechanical damping and unusual nonlinear behavior. We also discovered that a direct current through the nanotube spontaneously drives the mechanical resonator, exerting a force that is coherent with the high-frequency resonant mechanical motion.

---

\*Present address: Institute for Experimental and Applied Physics, University of Regensburg, 93040 Regensburg, Germany

Nanomechanical systems [1, 2] have promising applications, such as ultra-sensitive mass detection [3, 4, 5]. The combination of a high resonance frequency and a small mass also makes nanomechanical resonators attractive for a fundamental study of mechanical motion in the quantum limit [6, 7, 8, 9]. For a successful observation of quantum motion of a macroscopic object, a high-frequency nanoscale resonator must have low dissipation (which implies a high quality-factor  $Q$ ), and a sensitive detector with minimum back-action (i.e. quantum limited) [10, 11]. Here, we demonstrate a dramatic backaction that strongly couples a quantum dot detector to the resonator dynamics of a carbon nanotube, and which, in the limit of strong feedback, spontaneously excites large amplitude resonant mechanical motion.

Nanomechanical resonators have been realized by etching down larger structures. In small devices, however, surface effects impose a limit on the quality-factor [2]. Alternatively, suspended carbon nanotubes can be used to avoid surface damage from the (etching) fabrication process. We recently developed a mechanical resonator based on an ultra-clean carbon nanotube with high resonance frequencies of several 100 MHz and a  $Q$  exceeding  $10^5$  [12]. Here, we exploit this resonator to explore a strong coupling regime between single electron tunneling and nanomechanical motion. We followed the pioneering approaches in which aluminium single electron transistors were used as position detectors [6, 7, 8] and AFM cantilevers as resonators [13, 14, 15]; however, our experiment is in the limit of much stronger electro-mechanical coupling, achieved by embedding a quantum dot detector in the nanomechanical resonator itself.

Our device consists of a nanotube suspended across a trench that makes electrical contact to two metal electrodes (Fig. 1). Electrons are confined in the nanotube by Schottky barriers at the Pt metal contacts, forming a quantum dot in the suspended segment. The nanotube growth is the last step in the fabrication process, yielding ultra-clean devices [16], as demonstrated by the four-fold shell-filling of the Coulomb peaks (Fig. 1C). All measurements were performed at a temperature of 20 mK with an electron temperature of  $\sim 80$  mK.

We actuate the resonator with a nearby antenna, and detect the resonator motion by its influence on the d.c. current through the nanotube. The inset to Fig. 1D shows a peak in the current at the resonance frequency, which we have identified as a bending-mode mechanical resonance of the nanotube [12]. The  $Q$ -factor typically exceeds  $10^5$ , which is an increase of more than two orders of magnitude compared to previous nanotube studies [17, 18, 4]. The resonance frequency is tuned by more than a factor of 2 with the gate voltage (Fig. 1D). Here, the electric field from the gate voltage pulls the nanotube toward it, and the subsequent lengthening of the nanotube induces more tension, similar to the tuning of a guitar string [17].

Our detection signal results from a change in gate capacitance,  $\Delta C_g$ , during a displacement of the nanotube. This changes the effective quantum dot potential and, if positioned initially beside a Coulomb peak (Fig. 1C), can move it onto the peak, thereby increasing the current. For a nanotube oscillating on resonance, the effective potential oscillates, and the non-linearity of Coulomb blockade allows it to be rectified to a detectable d.c. current.

The narrow linewidth of the resonance peak due to the high  $Q$ -factor provides an unprecedented sensitive probe for studying nanomechanical motion. We first show the influence of a single electron on the resonance frequency,  $f_0$ . The Coulomb oscillations in Fig. 2A are caused by single electron tunneling giving rise to current peaks, and Coulomb blockade fixes the electron number in the valleys. From valley to valley, the electron number changes by one. Fig. 2B shows the mechanical resonance signal recorded at the same time. Overall, a more negative gate voltage (right to left) increases the total charge on the nanotube, increasing the tension. This process stiffens the mechanical spring constant and increases the resonance frequency. Linear stiffening occurs in the Coulomb valleys (indicated with dashed lines), whereas at Coulomb peaks, a peculiar softening occurs, visible as dips in  $f_0$ .

We first focus on the change in resonance frequency caused by the addition of one electron, which is measured as offsets of about 0.1 MHz between the dashed lines. This shift from single electron tuning, predicted in [19], is about 20 times our linewidth and thus clearly resolvable. Because we compare valleys with a fixed electron number, this single electron tuning comes from a change in a static force on the nanotube. The (electro-) static force is proportional to the square of the charge on the nanotube and thus adding one electron charge results, here, in a detectable shift in the mechanical resonance [19]. The shifts from single electron tuning can be as large as 0.5 MHz, more than 100 times the line width [20].

Next we focus on the dips in resonance frequency that occur at the Coulomb peaks. The current at the Coulomb peaks is carried by single electron tunneling, meaning that one electron tunnels off the nanotube before the next electron can enter the tube. The charge on the nanotube thus fluctuates by exactly one

electron charge,  $e$ , with a time dynamics than can be accounted for in detail by the theory of Coulomb blockade [21]. The average rate,  $\Gamma$ , at which an electron moves across the tube can be read off from the current  $I = e\Gamma$  (1.6 pA corresponds to a 10 MHz rate). Moving the gate voltage off or on a Coulomb peak, we can tune the rate from the regime  $\Gamma \sim f_0$  to  $\Gamma \gg f_0$  and explore the different effects on the mechanical resonance.

In Figs. 2A,B the Coulomb peak values of  $\sim 8$  nA yield  $\Gamma \sim 300f_0$ , the regime of many single electron tunneling events per mechanical oscillation. In addition to the static force and the radio frequency (RF) oscillating driving force, single electron tunneling now exerts a time-fluctuating, dynamic force on the mechanical resonator. We observe that this dynamic force causes softening, giving dips in the resonance frequency. The single electron charge fluctuations do not simply smooth the stepwise transition from the static single electron tuning shifts. Strikingly, fluctuations instead caused dips in the resonant frequency up to an order of magnitude greater than the single electron tuning shifts. As shown in [13, 22] and discussed in detail in the supporting online material [20], the dynamic force modifies the nanotubes spring constant,  $k$ , resulting in a softening of the mechanical resonance. The shape of the frequency dip can be altered by applying a finite bias,  $V_{sd}$ , across the nanotube. Starting from deep and narrow at small  $V_{sd} = 0.5$  mV, the dip becomes shallower and broader with increasing  $V_{sd}$ . This dip-shape largely resembles the broadening of Coulomb blockade peaks that occurs with increasing  $V_{sd}$ . We thus conclude from Fig. 2 that the single electron tuning oscillations are a mechanical effect that is a direct consequence of single electron tunneling oscillations.

Besides softening, the charge fluctuations also provide a channel for dissipation of mechanical energy. Fig. 3A shows the resonance dip for small RF power with frequency traces in Fig. 3B. In the Coulomb valleys, tunneling is suppressed ( $\Gamma \sim f_0$ ), damping of the mechanical motion is minimized, and we observe the highest Q-factors. On a Coulomb peak, charge fluctuations are maximal ( $\Gamma \gg f_0$ ), and the Q-factor decreases to a few thousand. These results explicitly show that detector backaction can cause significant mechanical damping. The underlying mechanism for the damping is an energy transfer occasionally occurring when a current-carrying electron is pushed up to a higher (electrostatic) energy by the nanotube motion before tunneling out of the dot. This gain in potential energy is later dissipated in the drain contact.

If we drive the system at higher RF powers (Fig. 3C,D) we observe an asymmetric resonance peak, along with distinct hysteresis between upward and downward frequency sweeps. Theoretically this marks the onset of non-linear terms in the equation of motion, such as in the well-studied Duffing oscillator [23, 24]. The spring constant,  $k$ , is modified by a large oscillation amplitude,  $x$ , which is accounted for by replacing  $k$  with  $(k + \alpha x^2)$ . The time-averaged spring constant increases if  $\alpha > 0$ , which is accompanied by a sharp edge at the high frequency side of the peak; vice versa for  $\alpha < 0$ . In addition to the overall softening of  $k$  yielding the frequency dips of Fig. 2, the fluctuating charge on the dot also changes  $\alpha$ , giving a softening spring ( $\alpha < 0$ ) outside of the frequency dip (Coulomb valleys), and a hardening spring ( $\alpha > 0$ ) inside the frequency dip (Coulomb peaks), shown in Fig. 3. The sign of  $\alpha$  follows the curvature of  $f_0(V_g)$  induced by the fluctuating electron force, giving a change in sign at the inflection point of the frequency dip. Interestingly, non-linearity from the single electron force in our device dominates, and is much stronger than that from the mechanical deformation [20].

Figs. 3E,F show the regime of further enhanced RF driving. The non-linearity is now no longer a perturbation of the spring constant, but instead gives sharp peaks in the lineshape and switching between several different metastable modes (see further data in supplementary material [20]). At this strong driving, we observe highly structured nonlinear mechanical behavior that arises from the coupling of the resonator motion to the quantum dot.

In figure 3, we studied non-linear coupling between the quantum dot and the mechanical resonator by applying a large RF driving force at a small Vsd. In figure 4, we consider a small or absent RF driving force and now apply a large Vsd across the quantum dot. Fig. 4A shows a standard Coulomb blockade measurement of the quantum dot. Mechanical effects in Coulomb diamonds have been studied before in the form of phonon sidebands of electronic transitions [25, 26, 27, 28]. Shown in the data of figure 4 are reproducible ridges of positive and negative spikes in the differential conductance as indicated by arrows. This instability has been seen in all 12 measured devices with clean suspended nanotubes and never in non-suspended devices. Fig. 4B and C shows such ridges in a second device, visible both as spikes in the differential conductance (Fig. 4B), and as discrete jumps in the current (Fig. 4C). The barriers in device 2 were highly tunable: we found that the switch-ridge could be suppressed by reducing the tunnel coupling to

the source-drain leads, thereby decreasing the current. The instability disappears roughly when the tunnel rate is decreased below the mechanical resonance frequency (see supporting online material)[20].

In a model predicting such instabilities [29], positive feedback from single electron tunneling excites the mechanical resonator into a large amplitude oscillation. The theory predicts a characteristic shape of the switch-ridges and the suppression of the ridges for  $\Gamma \sim f_0$ , in striking agreement with our observations. Such feedback also requires a very high Q, which may explain why it has not been observed in previous suspended quantum dot devices [26, 28]. If the required positive feedback is present, however, it should also have a mechanical signature: such a signature is demonstrated in Fig. 4E. The RF-driven mechanical resonance experiences a dramatic perturbation triggered by the switch-ridge discontinuities in the Coulomb peak current shown in Fig. 4D. At the position of the switch, the resonance peak shows a sudden departure from the expected frequency dip (dashed line), and becomes strongly asymmetric and broad, as if driven by a much higher RF power. This is indeed the case, but the driving power is now provided by an internal source: because of the strong feedback, the random fluctuating force from single electron tunneling becomes a driving force coherent with the mechanical oscillation. Remarkably, the d.c. current through the quantum dot can be used both to detect the high-frequency resonance and, in the case of strong feedback, directly excite resonant mechanical motion.

## References

- [1] H. G. Craighead, *Science* **290**, 1532 (2000).
- [2] K. L. Ekinci, M. L. Roukes, *Rev. Sci. Inst.* **76**, 061101 (2005).
- [3] K. L. Ekinci, X. M. H. Huang, M. L. Roukes, *Appl. Phys. Lett.* **84**, 4469 (2004).
- [4] B. Lassagne, D. Garcia-Sanchez, A. Aguasca, A. Bachtold, *Nano Lett.* **8**, 3735 (2008).
- [5] H.-Y. Chiu, P. Hung, H. W. Postma, M. Bockrath, *Nano Lett.* **8**, 4342 (2008).
- [6] R. G. Knobel, A. N. Cleland, *Nature* **424**, 291 (2003).
- [7] M. D. Lahaye, O. Buu, B. Camarota, K. C. Schwab, *Science* **304**, 74 (2004).
- [8] A. Naik, *et al.*, *Nature* **443**, 193 (2006).
- [9] K. C. Schwab, M. L. Roukes, *Phys. Today* **58**, 36 (2005).
- [10] C. M. Caves, K. S. Thorne, R. W. Drever, V. D. Sandberg, M. Zimmermann, *Rev. Mod. Phys.* **52**, 341 (1980).
- [11] C. A. Regal, J. D. Teufel, K. W. Lehnert, *Nature Phys.* **4**, 555 (2008).
- [12] A. K. Huettel, *et al.*, *Nano Letters* **9**, 2547 (2009).
- [13] M. T. Woodside, P. L. McEuen, *Science* **296**, 1098 (2002).
- [14] J. Zhu, M. Brink, P. L. McEuen, *Appl. Phys. Lett.* **87** (2005).
- [15] R. Stomp, *et al.*, *Phys. Rev. Lett.* **94**, 056802 (2005).
- [16] G. A. Steele, G. Gotz, L. P. Kouwenhoven, *Nature Nano.* **4**, 363 (2009).
- [17] V. Sazonova, *et al.*, *Nature* **431**, 284 (2004).
- [18] B. Witkamp, M. Poot, H. S. J. van der Zant, *Nano Lett.* **6**, 2904 (2006).
- [19] S. Sapmaz, Y. Blanter, L. Gurevich, H. S. J. van der Zant, *Phys. Rev. B* **67**, 235414 (2003).
- [20] Supporting online material available on *Science Online*.
- [21] C. W. J. Beenakker, *Phys. Rev. B* **44**, 1646 (1991).

- [22] M. Brink, thesis, Cornell Univerity (2007).
- [23] A. Cleland, *Foundations of Nanomechanics* (Springer-Verlag, 2002).
- [24] A. H. Nayfeh, D. T. Mook, *Nonlinear Oscillations* (Wiley, 1979).
- [25] H. Park, *et al.*, *Nature* **407**, 57 (2000).
- [26] S. Sapmaz, J. P. Herrero, Y. M. Blanter, C. Dekker, H. S. J. van der Zant, *Phys. Rev. Lett.* **96** (2006).
- [27] F. A. Zwanenburg, C. E. van Rijmenam, Y. Fang, C. M. Lieber, L. P. Kouwenhoven, *Nano Lett.* **9**, 1071 (2009).
- [28] R. Leturcq, *et al.*, *Nature Phys.* **5**, 327 (2009).
- [29] O. Usmani, Y. M. Blanter, Y. V. Nazarov, *Phys. Rev. B* **75**, 195312 (2007).

### **Acknowledgments**

We thank Y. M. Blanter and Y. V. Nazarov for helpful discussions. This work was supported by the Dutch Organization for Fundamental Research on Matter (FOM), the Netherlands Organization for Scientific Research (NWO), the Nanotechnology Network Netherlands (NanoNed), and the Japan Science and Technology Agency International Cooperative Research Project (JST-ICORP).

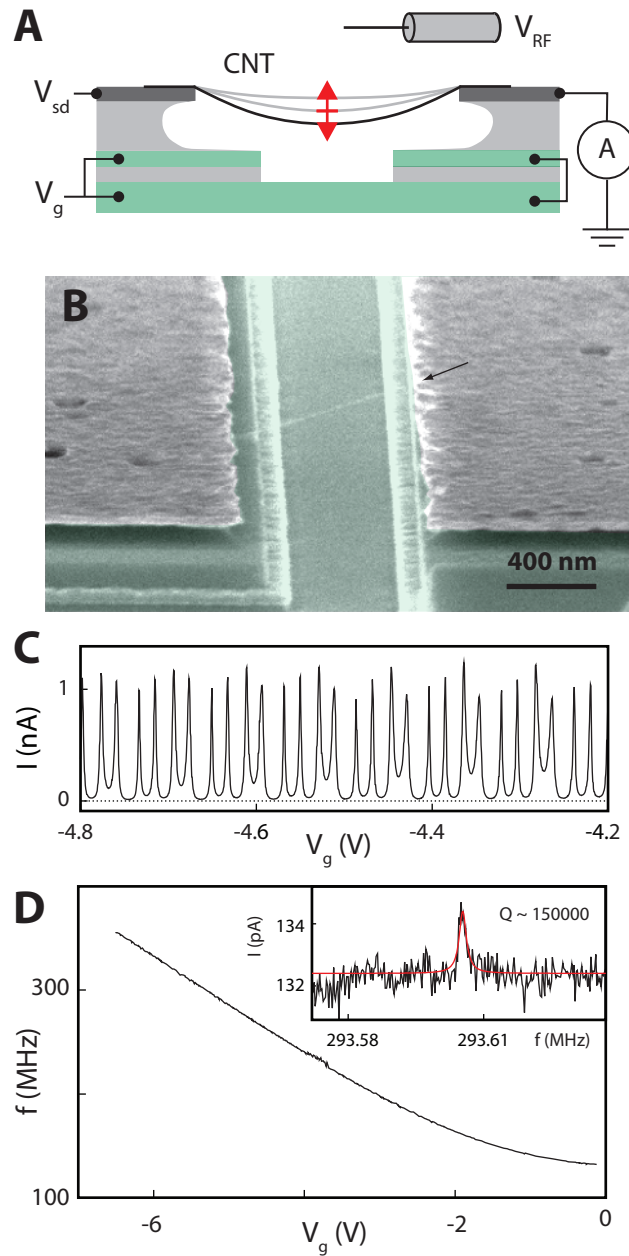


Figure 1: A high quality-factor nanotube mechanical resonator with an embedded quantum dot. (A) Device layout. A suspended carbon nanotube is excited into mechanical motion by applying an a.c. voltage to a nearby antenna. A d.c. current through the nanotube detects the motion.  $V_{RF}$ , radio frequency voltage; CNT, carbon nanotube. (B) SEM image of a typical device. (C) A quantum dot, formed between Schottky barriers at the metal contacts, displays 4-fold shell filling of holes. (D) (Inset) The mechanical resonance induces a corresponding resonance in the d.c. current which can have a narrow linewidth with quality-factors up to 150 000. (Main plot) The resonance frequency can be tuned using a tensioning force from the d.c. voltage on the gate.

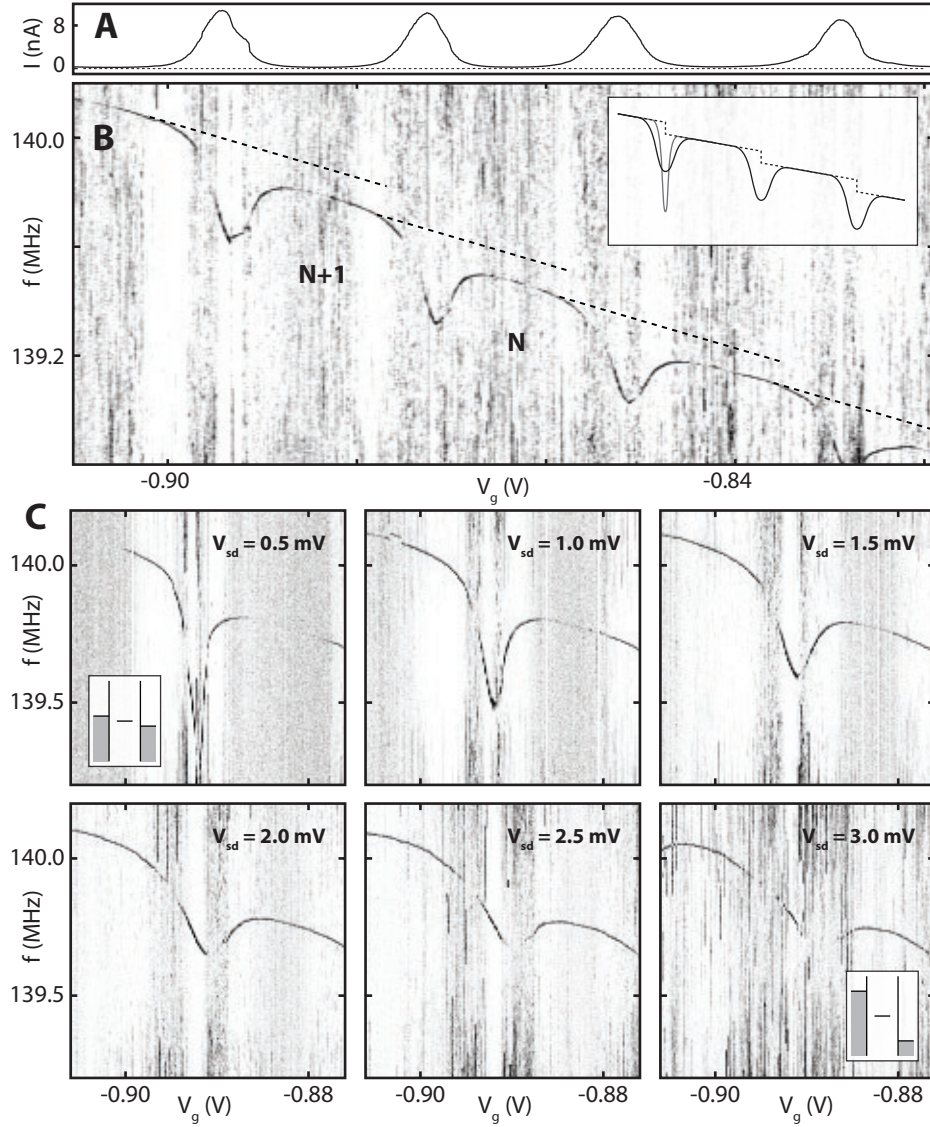


Figure 2: Single electron tuning. (A) Nanotube current vs. gate voltage showing single electron tunneling at the peaks and Coulomb blockade in the valleys. This curve is taken from (B) at  $f = 138.8$  MHz. (B) Normalized resonance signal  $\Delta I / \Delta I_{peak}$  (see supporting online material) vs. RF frequency and gate voltage ( $V_{sd} = 1.5$  mV). The tuned mechanical resonance shows up as the darker curve with dips at the Coulomb peaks. The offsets between dashed lines indicate the frequency shift due to the addition of one electron to the nanotube. The resonance frequency also shows dips caused by a softening of the spring constant due to single electron charge fluctuations.  $N$ , number of holes on the quantum dot. (Inset) The expected resonance behavior (see text). (C) Zoom on one frequency dip for various source-drain voltages ( $V_{sd}$ ) showing dip broadening for increasing  $V_{sd}$ . (Insets) Energy diagrams for small and large  $V_{sd}$ .

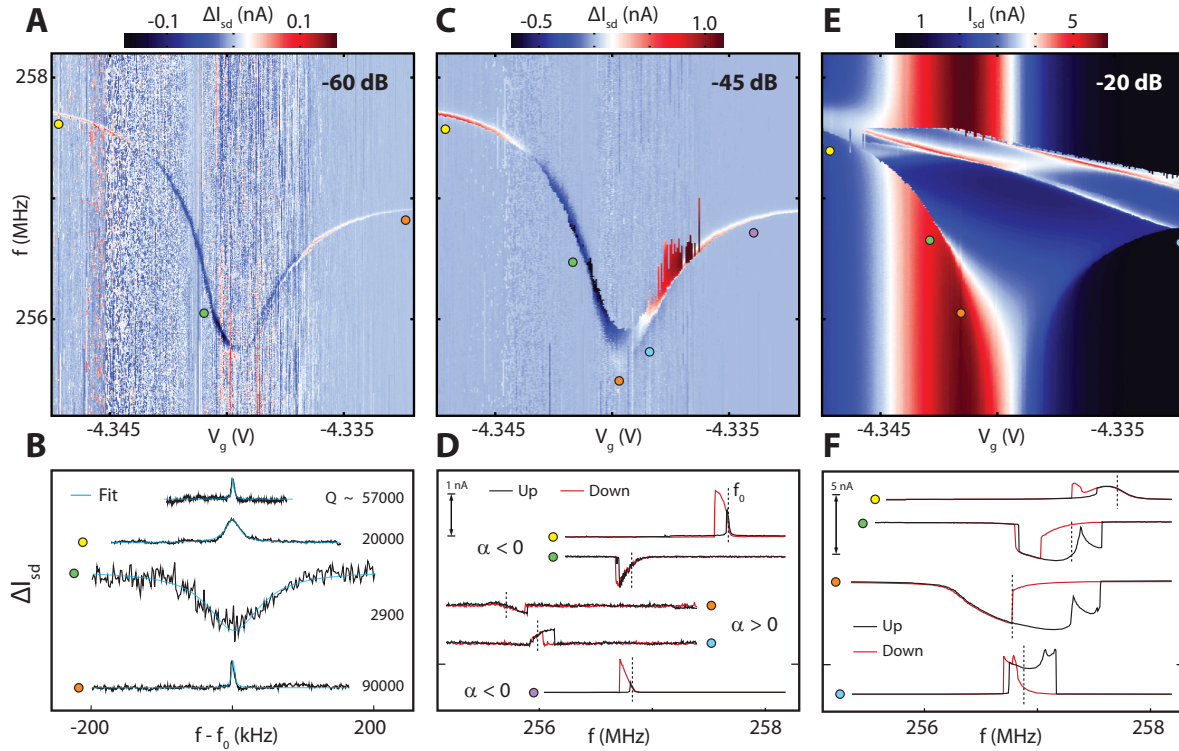


Figure 3: Lineshapes of the mechanical resonance from linear to non-linear driving regimes. (A) Detector current ( $\Delta I$ ) vs. frequency and gate-voltage at RF excitation power of -60 dB as the gate voltage is swept through one Coulomb peak. (B) Fits of the resonance to a squared Lorentzian lineshape at different gate voltages [12]. The RF power for each trace is adjusted to stay in the linear driving regime (-75,-64,-52, and -77 dB top to bottom). Traces are taken at the positions indicated by colored circles (aside from the top trace which is taken at  $V_g = -4.35$  V). (C) At -45 dB, the resonance has an asymmetric lineshape with one sharp edge, see linecuts (D), typical for a non-linear oscillator [23, 24]. Dashed lines in (D) and (F) indicate resonance frequency  $f_0$  at low powers. (E) and (F) At even higher driving powers (-20 dB), the mechanical resonator displays sharp sub-peaks and several jumps in amplitude when switching between different stable modes. (C) and (E) are taken in the upwards sweep direction (downwards sweeps shown in supporting online material).

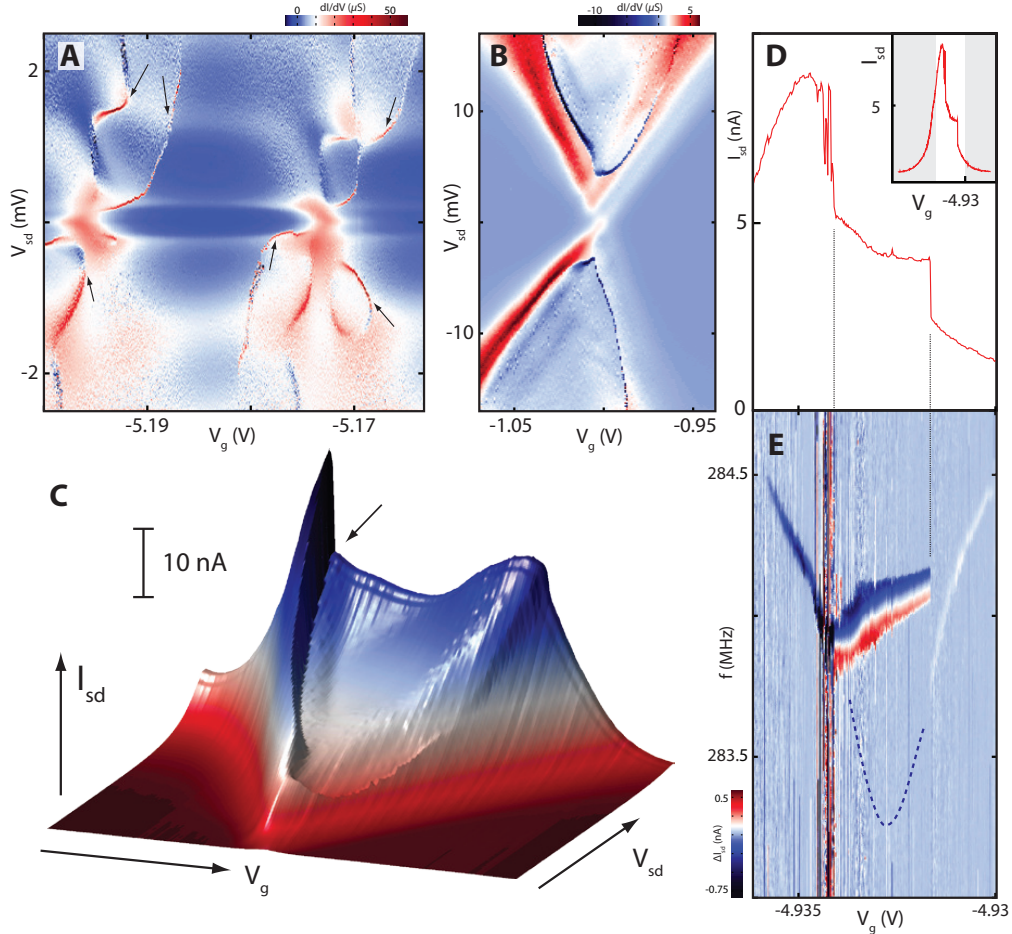


Figure 4: Spontaneous driving of the mechanical resonance by single-electron tunneling. (A) Differential conductance,  $dI/dV_{sd}$ , showing ridges of sharp positive (deep red) and negative (deep blue) spikes (arrows). (B) Similar ridges measured on device 2 (trench width = 430 nm) in the few-hole regime (4hole to 3hole transition). Spikes in  $dI/dV_{sd}$  appear as step-like ridges in current: (C) shows the data from the upper half of (B), but now as a 3D current plot. Note that the ridges are entirely reproducible. (D) Inset: Coulomb peak at  $V_{sd} = 0.5$  mV showing large switching-steps. Main plot: zoom-in on data from inset. (E) RF driven mechanical resonance measured for the same Coulomb peak in (D) at a driving power of -50 dB. Outside the “switch-region”, the resonance has a narrow lineshape and follows the softening-dip from Figs. 2,3. At the first switch, the resonance position departs from the expected position (indicated by dashed line). The mechanical signal is strongly enhanced in amplitude and displays a broad asymmetric lineshape. At the second switch, the resonance returns to the frequency and narrow lineshape expected at these powers.